# Synthesis of Pt nanowires inside aerosol derived spherical mesoporous silica particles

Mangesh T. Bore[1], Timothy L. Ward[1], Atsushi Fukuoka[2], and Abhaya K. Datye[1,]*

[1]*Department of Chemical and Nuclear Engineering, Ceramic and Composite Materials Center, University of New Mexico, Albuquerque, NM 87131, USA*

[2]*Hokkaido University, Sapporo 060-0811, Japan*

Received 20 July 2004; accepted 10 September 2004

Spherical mesoporous silica particles prepared by evaporation induced self assembly (EISA) were used as templates to form Pt nanowires. Transmission electron microscope (TEM) images of these aerosol-derived silica particles reveal hexagonally ordered pores coiled within each particle, with no obvious termination of the pores on the external surface. Near the particle surface the pores are seen to run parallel to the surface, consistent with the external constraint of spherical geometry. For MCM-41 type mesoporous materials, the pores are straight and accessible at either end for pore filling, but for spherical silica particles prepared by EISA, the pores are not open to the external surface. Hence it is remarkable that Pt nanowires can be formed within the closed pores inside these spherical silica particles, where conventional mechanisms of pore filling would not be expected to be operative. These results suggest that the silica walls in these mesoporous silica allow transport of volatile Pt complexes during wet reduction in $H_2$. The permeability to gases makes these spherical silica particles especially suitable for gas phase catalytic reactions, while at the same time confining metallic particles within the silica pores.

**KEY WORDS**: platinum nanowires; mesoporous silica; evaporation induced self assembly; novel catalyst.

## 1. Introduction

Mesoporous silica with pores in the size range of 2–10 nm has recently been used as template for the synthesis of nanowires [1–6]. The silica powder is generally produced via surfactant templated self assembly following an approach pioneered by Kresge *et al.* [7] which involves batch synthesis using an autoclave. The process is conducted over a time scale of days or longer to ensure a high degree of order in the final inorganic product. The metal nanowires are formed by filling of the pores through various means including chemical reduction of metal complexes, supercritical pore filling, etc. In this paper, we report an alternative approach for the synthesis of the silica template, based on evaporation induced self assembly (EISA) [8,9] where an aerosol of droplets of the precursor solution are passed through a furnace. The aerosol method can produce highly ordered mesoporous oxide particles with a total process time of a few seconds or less, much shorter than the typical time scale used for the conventional batch approach. For the synthesis of mesoporous powders, EISA of aerosols has several other very attractive features compared to traditional bulk solution methods. The process is a continuous, scaleable process that can make spherical particles over a fairly wide size range. By using a vibrating orifice aerosol generator (VOAG), monodisperse silica particles can also be produced [10]. The hydrothermal stability of the silica backbone can be improved by addition of heteroelements (Bore *et al.*, submitted) such as Al or Zr.

The mesoporous silica particles produced by surfactant templates using the aerosol method are spherical and have hexagonally ordered pores. Transmission electron microscope (TEM) images of mesoporous silica particles produced by the aerosol route (figure 1) show two types of regions, region “A” where hexagonally ordered pores are imaged end-on and region “B” where the pores are parallel to the surface. Both of these regions “A” and “B” arise from the same structure but differ only in terms of their orientation with respect to the electron beam. For instance, region “A” will give rise to an image similar to region “B” if the particle is imaged along the arrowed direction in figure 1. We have concluded that these particles consist of hexagonally ordered pores coiled up so that they fit within the spherical geometry. None of the TEM images show any pores coming out perpendicular to the surface of particle, and it appears at first glance these pores are inaccessible. However, the internal silica surface is accessible, at least to $N_2$ gas, since the measured BET surface area is 1010 $m^2/g$. Figure 2 shows the nitrogen adsorption isotherm. The pore structure of these spherical particles is very different from that of conventional MCM-41 [7] where the hexagonally ordered pores are straight and

---

*To whom correspondence should be addressed.
E-mail: datye@unm.edu

1011-372X/04/1200–0167/0

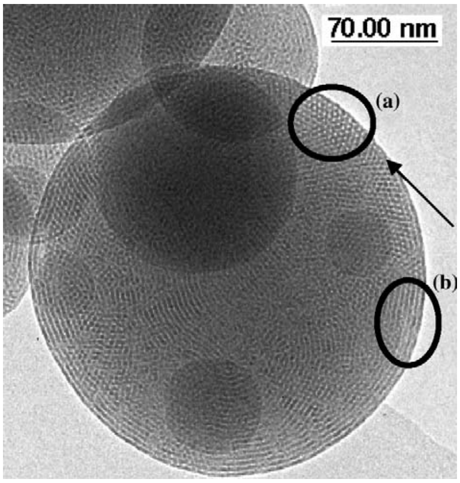

Figure 1. Transmission electron microscope (TEM) image of mesoporous silica particles produced by evaporation induced self assembly. The particles are spherical with mesopores running parallel to the surface of the sphere. The two orientations A and B correspond to pores running perpendicular or parallel to the plane of the image, but otherwise these pores are indistinguishable. (Reproduced with permission from Langmuir, 19 (2003) 256–264. Copyright 2003 Am. Chem. Soc.).

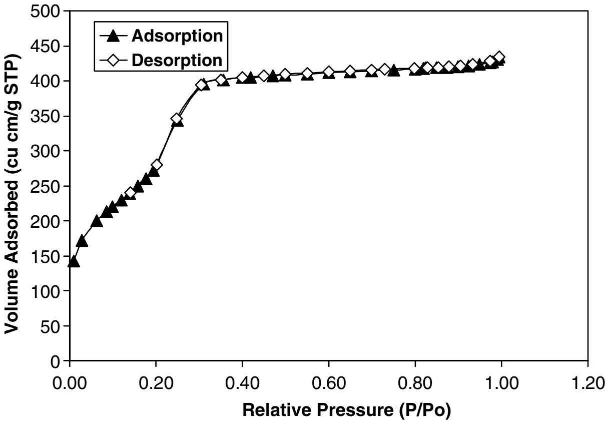

Figure 2. Nitrogen adsorption isotherm for aerosol synthesized mesoporous silica particles.

accessible at either end for pore filling. It was therefore of interest to see whether Pt nanowires could be formed within the pores of spherical silica particles.

## Experimental

Mesoporous silica particles were produced using a TSI 3076 aerosol generator. The precursor solution consisted of cetyltrimethyl ammonium bromide (CTAB), water, tetraethylorthosilicate (TEOS) and 1 N hydrochloric acid. The molar ratio of TEOS : $H_2O$ : CTAB : HCl used was 1 : 63 : 0.16 : 0.02. The precursor solution was passed through an aerosol reactor. The furnace temperature was maintained at 425 °C. The powder collected on a filter paper was subsequently calcined at 500 °C for 12 h in air to remove the surfactant. A detailed description of the synthesis of mesoporous silica particles with four aerosol generators has been published elsewhere [9]. For the synthesis of nanowires, we took 200 mg of aerosol generated silica particles and mixed them with an aqueous solution of 28 mg of $H_2PtCl_6 \cdot 6H_2O$ in 30 ml water. After 24 h of stirring, the solution was vacuum dried for another 24 h. The powder after vacuum drying was termed the "as-prepared" sample.

## Results and discussion

Figure 3 (a, b) shows high angle annular dark field (HAADF) STEM images of the as-prepared sample. In this imaging mode, image brightness is related to atomic number or sample thickness. Energy dispersive spectroscopy (EDS) was used to quantify the Pt/silica ratio in these samples (figure 3c, d). EDS mapping revealed that the Pt was uniformly distributed within the silica samples. The overall Pt loading by EDS analysis was calculated as 4.8 wt%, which is close to expected Pt loading based on the amounts of precursor solution used. It was found that the Pt was uniformly distributed throughout the sample. What is seen in figure 3 are mainly the silica pores, with few bright dots representing Pt particles that have formed due to electron beam induced reduction of the precursor chloroplatinic acid.

The as-prepared Pt/silica powder was reduced in flowing $H_2$ under "wet" or 'dry' conditions. In the 'dry' reduction process, the as-prepared sample was reduced at 200 °C for 2 h (ramp rate used was 0.73 °C/min) in presence of 100% hydrogen. The 'wet' reduction was performed in flowing $H_2$ saturated with water vapor at 200 °C for 2 h with the same ramp rate. HAADF images after dry-reduction (figure 4) show the presence of Pt nanoparticles co-existing with some Pt-nanowires. While the majority of the Pt formed nanoparticles, it is clear that some nanowires formation was also initiated during the dry-reduction step. Figure 5 presents an SEM image of this sample after wet reduction. The image on the right (figure 5b) is a back scattered electron image that shows that the Pt nanowires have formed in only a few of the particles. This observation is confirmed by the HAADF images obtained in the STEM (figure 6). Extensive formation of Pt nanowires is seen inside only a small number of particles of mesoporous silica. Pt nanowires follow the pores and clearly reveal the internal pore structure in these mesoporous silica particles. Pores are locally hexagonally ordered but then they change direction and are coiled throughout the particle to confirm to the spherical shape of the particle. It is also interesting that none of the Pt nanowires seem to terminate on the particle surface.

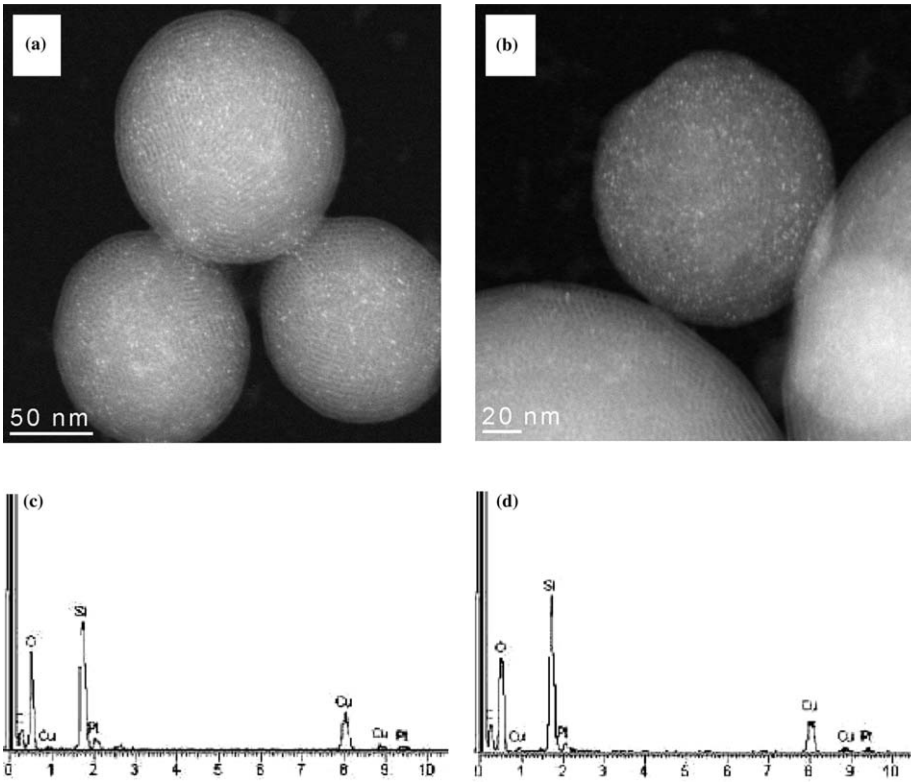

Figure 3. High angle annular dark field (HAADF) images (a, b) in a scanning transmission electron microscope (STEM) of the Pt/silica sample after impregnation with chloroplatinic acid and drying in vacuum. In these images, we see the pores of mesoporous silica, with bright dots that correspond to Pt nanoparticles that may have nucleated due to reduction to metallic Pt during electron beam exposure. "c" and "d" are EDS patterns for images "a" and "b" respectively.

The TEM image involves a 2-D projection of a 3-D sample; hence there is considerable overlap in the nanowire images seen in TEM. We also studied these samples with high resolution SEM at an accelerating voltage of 1 kV, where the limited penetration depth ensures that only the sample surface is being imaged. The SEM images are shown in figure 6 where we can see the morphology of the nanowires (and hence the mesopores) in this silica sample. The images show that the nanowires do indeed run along the surface in bundles, in a swirl like pattern. In these images, we do not see any of the nanowires running end-on into the surface of the sample, in which case we should see just the ends of the nanowires in the form of bright dots on the sample surface.

It is evident that after 'wet' reduction, the Pt has segregated to a few of the spheres, while the majority of the silica particles show no Pt to be present at all (figure 5). This is in contrast to the Pt distribution in the as-prepared catalyst, or after "dry" reduction, when the Pt was found to be present uniformly throughout the sample (Figures 3 and 4). The fact that Pt nanowires are present only on few of the spheres suggests that during "wet" reduction, the Pt species must be mobile enough that Pt can move freely from one particle to another. We suggest that Pt reduction is initiated at a few nucleation sites. and nanowires form by adding Pt species to these nuclei. Since the pore structure of these silica spheres does not show direct termination of the pores on the surface of the particle, we suggest that the silica walls must be permeable to gas phase species that lead to transport of Pt during the "wet" reduction. The permeability of the silica could be caused by defects that are not visible in the TEM images. It is well known that volatile Pt species are formed when Pt catalysts are treated in a chlorine and oxygen atmosphere and the redistribution of Pt is used to regenerate catalysts that have sintered to fom1 large Pt particles [11]. In our case, we start with chloroplatinate anions which in the presence of wet $H_2$ appear to form similar volatile Pt complexes. Such volatile complexes may not form without the presence of water vapor, since during "dry" reduction we see primarily the presence of Pt nanoparticles. The presence of microporosity in the pore walls was ruled out by the $\alpha_s$-plot analysis and $wS/V$ ratio [12] ($w$: pore size 30.6 Å, $S$: surface area 1010 $m^2/g$, $V$: pore volume 0.659 $cm^3/g$, $wS/V$ ratio = 4.6). These spherical silica particles fulfilled the fundamental relation between the standard parameters for materials with uniform pores of simple circular or hexagonal geometry: $wS/V$ = 4 or 4.2, respectively. The initial part of the $\alpha_s$-plot [13]

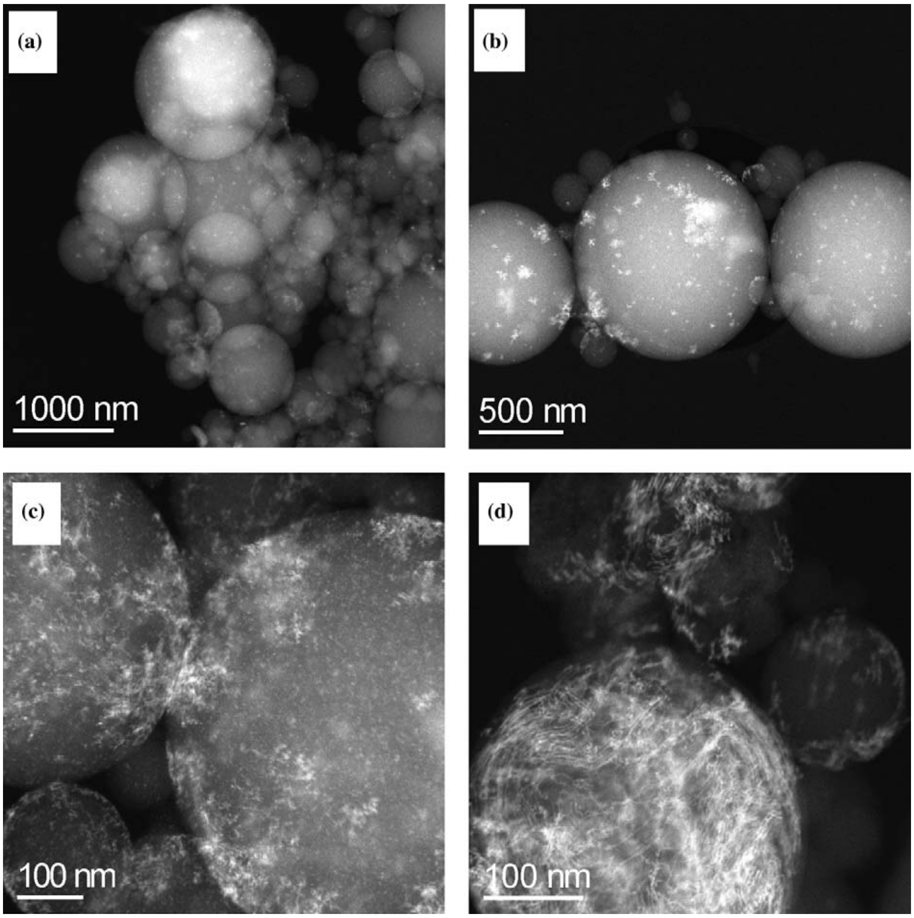

Figure 4. HAADF STEM images of the Pt/silica sample after reduction in pure hydrogen at 200 °C for 2 h (dry-reduction). We see mostly Pt nanoparticles (a–c). but in a few regions it is evident that Pt nanowire formation has also been initiated (d).

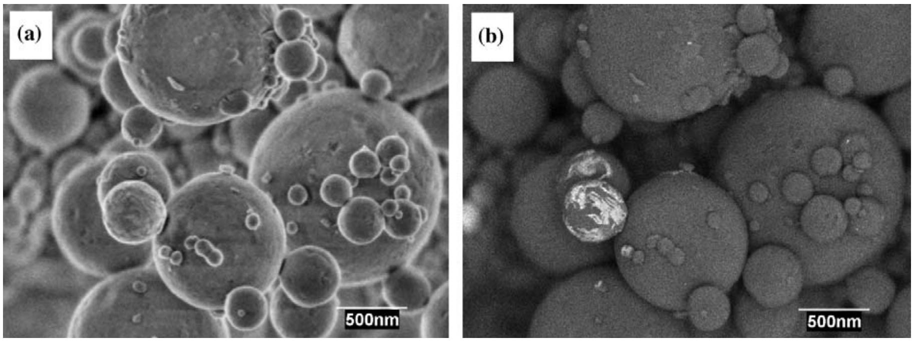

Figure 5. SEM image (1 kV) of the Pt/silica after wet reduction. The secondary electron image on the left (a) shows the sample morphology while the back scattered electron image on the right (b) shows that the bright Pt wires are present in only a few particles, while others appear to be devoid of Pt.

(figure 8) calculated from nitrogen adsorption isotherm data was linear, confirming absence of micropores in the silica walls. Hence we infer that the volatile Pt species must either diffuse through walls of silica particles or that these silica particles have defects that permit facile transport of gas phase species. It is clear that these silica particles are permeable to $N_2$ since the measured surface area of 1010 $m^2/g$ is consistent with that seen in MCM-41 silica where the pores run in hexagonal bundles with the pore mouths open to the gas phase. The ease with which we can reduce the Pt species in $H_2$ suggests that the silica must also be permeable to gas phase $H_2$. The accessibility and permeability of these Pt nanowires silica samples suggest that they would make interesting heterogeneous catalysts. Indeed, these catalysts show high activity for oxidation of gas phase CO.

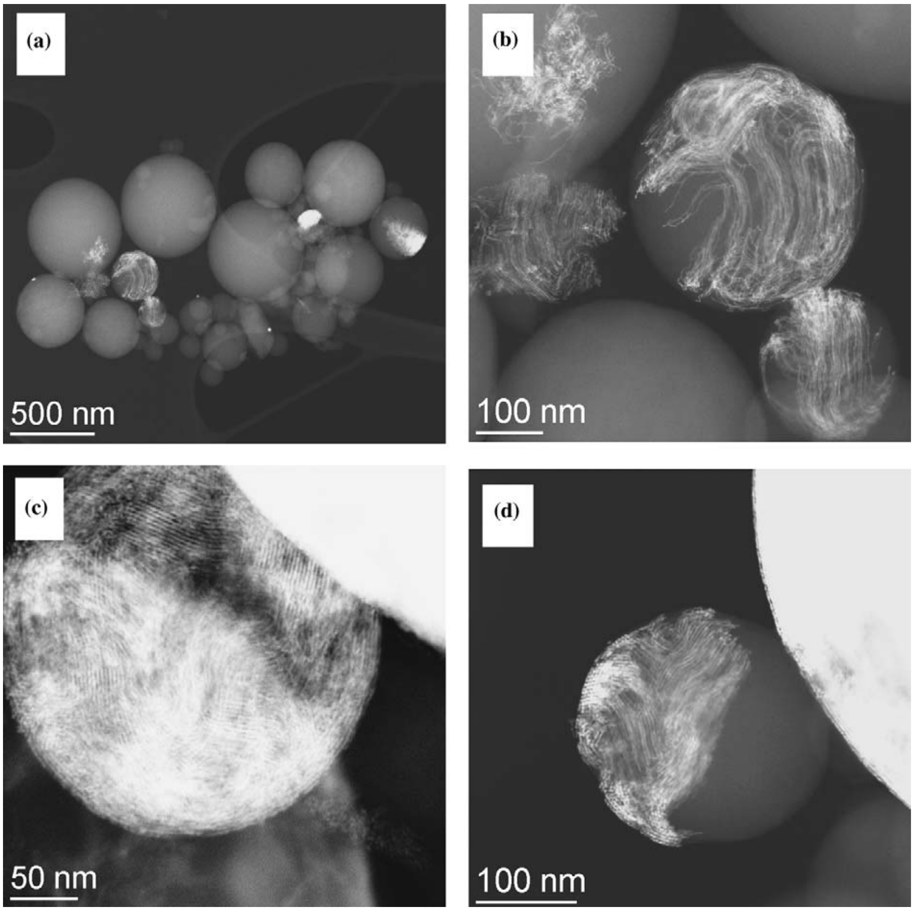

Figure 6. HAADF STEM images of sample after reduction in hydrogen saturated with water vapor at 200 °C for 2 h (wet-reduction). Pt nanowires can be seen in only a few of the spheres, there are no Pt nanoparticles seen in this sample.

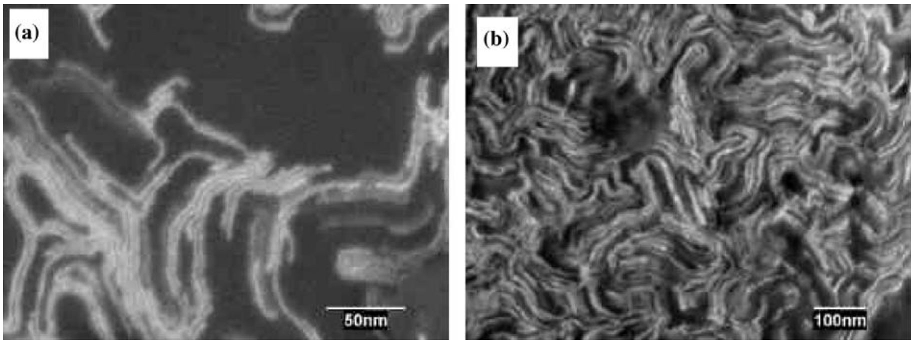

Figure 7. High resolution SEM images of Pt nanowires imaged at 1 kV. Due to the limited penetration depth at this low voltage, we see only the topmost layer of the Pt nanowires. The Pt nanowires are seen to follow a swirl-like pattern, folding over into lamellar regions. Almost none of the pores terminate on the silica surface end-on.

## Conclusions

In conclusion, we have demonstrated that Pt-nanowires can be synthesized inside the closed pores of aerosol generated mesoporous silica particles. The Pt was uniformly distributed through the silica after impregnation. After dry reduction, the Pt formed nanoparticles were distributed uniformly throughout the sample. Only after wet reduction did we see extensive fomulation of Pt nanowires. This is consistent with the work of Fukuoka *et al.* [5,14] where migration of Pt species was shown to be an important step for formation of Pt nanowires. Though Pt was uniformly distributed

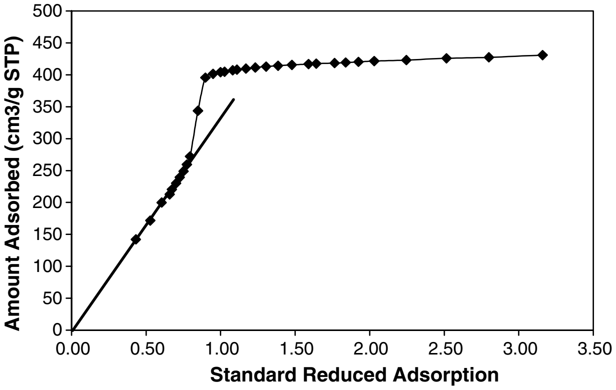

Figure 8. $\alpha_s$-plot for aerosol synthesized mesoporous silica particles.

all over silica particles in the initial as-prepared state, after wet-reduction Pt-nanowires were found only in a few of the silica particles. The aspect ratio of the nanowires (length/diameter ratio) suggests that mobile Pt species are able to nucleate at the tip and continue to form within the silica mesopores. Since Pt is localized in a few particles, we suggest that these mesoporous silica particles allow facile transport of gas phase species either due to thin silica walls or the presence of defects in the silica framework. The Pt nanowires also allow us to clearly visualize the internal pore structure of the silica spheres.

## Acknowledgments

We acknowledge support of this research by the US National Science Foundation grants CTS 02-10835. EEC 99-08205 and the Materials Corridor Council supported by the Department of Energy. The SEM used in this work was acquired through the New Mexico NSF EPSCOR infrastructure grant. AF thanks the Ministry of Education, Science. Sports and Culture, Japan for the support of a sabbatical visit to New Mexico.

## References

[1] C.H. Ko and R. Ryoo, Chem. Comm. 21 (1996) 2467.

[2] Y.-J. Han, J.M. Kim and G.D. Stucky, Chem. Mater. 12 (2000) 2068.

[3] M.H. Huang, A. Choudrey and P. Yang, Chem. Comm. 12 (2000) 1063.

[4] N.R.B. Coleman, M.A. Morris, T.R. Spalding and J.D. Holmes, J. Am. Chem. Soc. 123 (2001) 187.

[5] A. Fukuoka, H. Araki, Y. Sakamoto, N. Sugimoto, H. Tsukada, Y. Kumai, Y. Akimoto and M. Ichikawa, Nano Lett. 2 (2002) 793.

[6] J. Liu, G.E. Fryxell, M. Qian, L.Q. Wang and Y. Wang, Pure Appl. Chem. 72 (2000) 269.

[7] C.T. Kresge, M.E. Leonowicz, W.J. Roth, J.C. Vartuli and J.S. Beck, Nature 359 (1992) 710.

[8] Y. Lu, H. Fan, A. Stump, T.L. Ward, T. Rieker and C.J. Brinker, Nature 398 (1999) 223.

[9] M.T. Bore, S.B. Rathod, T.L. Ward and A.K. Datye, Langmuir 19 (2003) 256.

[10] G.V.R. Rao, G.P. Lopez, J. Bravo, H.N. Pham, A.K. Datye, H.F. Xu and T.L. Ward, Adv. Mater. 14 (2002) 1301.

[11] S.C. Fung, Catal. Deactiv. Proc. 139 (2001) 399.

[12] R. Ryoo, C.H. Ko, M. Kruk, V. Antochshuk and M. Jaroniec, J. Phys. Chem. B 104 (2000) 11465.

[12] M. Kruk, M. Jaroniec and A. Sayari, Langmuir 13 (1997) 6267.

[14] Y. Sakamoto, A. Fukuoka, T. Higuchi, N. Shimomura, S. Inagaki and M. Ichikawa, J. Phys. Chem. B 108 (2004) 853.